Electronic Supplementary Material (ESI) for Journal of Materials Chemistry A.
This journal is © The Royal Society of Chemistry 2021

Supporting Information

All-Polymer Solar Cell with Efficiency Approaching 16% Enabled by Dithieno[3',2':3,4;2'',3'':5,6]benzo[1,2-c][1,2,5]thiadiazole (fDTBT)-Based Polymer Donor

Tao Jia,[‡a] Jiabin Zhang,[‡a] Kai Zhang*[a], Haoran Tang,[a] Sheng Dong,[a] Ching-Hong Tan,[a] Xiaohui Wang*[a] and Fei Huang*[a]

[*] *Corresponding authors*

[a] *Institute of Polymer Optoelectronic Materials and Devices, State Key Laboratory of Luminescent Materials and Devices, and State Key Laboratory of Pulp & Paper Engineering, South China University of Technology, Guangzhou 510640, China. E-mail: mszhangk@scut.edu.cn; fewangxh@scut.edu.cn; msfhuang@scut.edu.cn*

[‡] *These authors contributed equally to this work.*

Experimental Section

Materials

The commercial BDT-based monomers (4,8-bis(5-(2-ethylhexyl)thiophen-2-yl)benzo[1,2-b:4,5-b']dithiophene-2,6-diyl)bis(trimethylstannane) (DSn-BDT), (4,8-bis(5-((2-ethylhexyl)thio)thiophen-2-yl)benzo[1,2-b:4,5-b']dithiophene-2,6-diyl)bis(trimethylstannane) (DSn-BDT-S), (4,8-bis(5-(2-ethylhexyl)-4-fluorothiophen-2-yl)benzo[1,2-b:4,5-b']dithiophene-2,6-diyl)bis(trimethylstannane) (DSn-BDT-F), and (4,8-bis(5-((2-ethylhexyl)thio)-4-fluorothiophen-2-yl)benzo[1,2-b:4,5-b']dithiophene-2,6-diyl)bis(trimethylstannane) (DSn-BDT-S-F) are purchased from Solarmer Materials Inc. The tributyl(4-(2-butyloctyl)thiophen-2-yl)stannane,[1] PJ1,[2] and PNDIT-F3N-Br[3] were synthesized according to the procedure reported. Other chemicals and solvents are purchased from J&K, Alfa Aesar and TCI Chemical Co., respectively.

Synthetic Procedures

Synthesis of 5,8-bis(5-bromo-4-(2-butyloctyl)thiophen-2-yl)dithieno[3',2':3,4;2'',3'':5,6]benzo[1,2-c][1,2,5]thiadiazole (M1)

To a two-neck flask containing compound 1 (4.06 g, 10 mmol), tributyl(4-(2-butyloctyl)thiophen-2-yl)stannane (8.12g, 30 mmol), and dried toluene (75 ml) was added $Pd(PPh_3)_4$ (575 mg) under N_2 atmosphere. The reaction mixtures were stirred vigorously at 100 °C for 18 h. After cooled to room temperature, the organic phase was removed by reduced pressure and the residue was purified by a fast column chromatography on silica gel to afford compound 2 (7.04g, yield 94%) as yellow solid that was directly used for the next brominated reaction. Compound 2 (3.75g, 5mmol) was dissolved in 75 mL chloroform in a 150 mL flask and the N-Bromosuccinimide (1.71g, 9.6 mmol) was added in three pots within one hour. The reaction was kept stirring for 3 h at room temperature. After that, the reaction mixture was poured into water and the organic phase was collected. After the removal of solvent, the crude product was purified by a fast column chromatography on silica gel using petroleum ether (PE) / dichloromethane (DCM) (2/1, *v/v*) as the eluent to afford the residue M1. The residue M1 was further recrystallized with hot DCM/MeOH(5/1, *v/v*) for three times to yield M1 as yellow solid. (4.08 g, yield 90%). ^{1}H NMR (500 MHz, $CDCl_3$): δ 7.63 (s, 2H), 6.84 (s, 2H), 2.47 (d, J = 7.2 Hz, 4H), 1.69 (s, 2H), 1.35 – 1.27 (m, 30H), 0.91 (dt, J = 13.6, 6.8 Hz, 12H). ^{13}C NMR (126 MHz, $CDCl_3$) δ 149.80, 142.49, 136.56, 135.48, 132.90, 129.25, 126.09, 119.16, 110.19, 38.53, 34.21, 33.34, 33.04, 31.95, 29.74, 28.78, 26.53, 23.11, 22.74, 14.20, 14.18.

The universal synthetic procedures for the target donor polymers:

Compound M1 (270.1 mg, 0.3 mmol), BDT-based monomers (0.3 mmol), $Pd_2(dba)_3$ (5.4 mg) and P (*o*-tol)$_3$ (8.1 mg) were combined in a 48 mL sealed tube. Dry chlorobenzene (CB) (15 mL) was added under the argon atmosphere. The reaction mixture was stirred vigorously at 140 °C for 36 h. Then the hot reactant mixture was immediately poured into methanol (MeOH) (300 mL), resulting in precipitation. The precipitate was filtered and Soxhlet extracted with methanol, hexane, dichloromethane, chloroform and chlorobenzene. The ingredient extracted from chlorobenzene was concentrated, precipitated into methanol, filtered and dried under vacuum to give the red fiber solid.

JD40: 86% yield; M_n = 49.7 kDa, M_w = 124.5 kDa; ^{1}H NMR (600 MHz, $C_2D_2Cl_4$, 120 ^{o}C): δ 8.15 – 8.12 (m, 2H), 7.79 – 7.77 (m, 2H), 7.45 (m, 2H), 7.28 – 7.26 (m, 2H), 7.03 – 7.00 (m, 2H), 3.01 (m, 4H), 2.90 (m, 4H),1.88 – 1.84 (m, 4H), 1.59 – 1.55 (m, 4H), 1.48 – 1.43 (m, 20H), 1.38 – 1.34 (m, 24H), 1.09 – 1.04 (m, 12H), 0.96 – 0.93(m, 12H).

JD40-S: 88% yield; M_n = 51.2 kDa, M_w = 123.8 kDa; ^{1}H NMR (600 MHz, $C_2D_2Cl_4$, 120 ^{o}C): δ 8.16 – 7.90 (m, 2H), 7.73 – 7.58 (m, 2H), 7.47 – 7.44 (m, 2H), 7.35 – 7.33 (m, 2H), 7.29 – 6.98 (m, 2H), 3.16 –3.06 (m, 4H), 2.88 –2.66 (m, 4H), 1.85 (m, 4H), 1.66 – 1.62 (m, 8H), 1.45 – 1.35 (m, 40H), 1.10 – 0.95 (m, 24H).

JD40-F: 81% yield; M_n = 57.2 kDa, M_w = 112.7 kDa; ^{1}H NMR (600 MHz, $C_2D_2Cl_4$, 120 ^{o}C): δ 8.17 – 7.78 (m, 4H), 7.55 – 7.47 (m, 2H), 7.29 – 7.03 (m, 4H), 3.00-2.94 (m, 8H), 1.91 – 1.83 (m, 4H), 1.62 – 1.56 (m, 12H), 1.44 – 1.35 (m, 34H),1.17 – 1.04 (m, 12H), 0.97 – 0.94 (m, 12H).

JD40-S-F: 78% yield; M_n = 42.2 kDa, M_w = 96.5 kDa; ^{1}H NMR (600 MHz, $C_2D_2Cl_4$, 120 ^{o}C): δ 8.17 – 7.48 (m, 6H), 7.35 – 7.12 (m, 4H), 3.06-2.90 (m, 8H), 1.86 – 1.77 (m, 4H), 1.63 (m, 8H), 1.44 – 1.39 (m, 40H), 1.05 – 0.95 (m, 24H).

Instruments and Measurement

^{1}H NMR and ^{13}C NMR spectra were measured on a Bruker AV-500 MHz or Bruker AVANCE III 600 MHz spectrometer with tetramethylsilane (TMS) as the internal reference. Molecular weights of the polymers were obtained on an Acquity Advanced Polymer Chromatography (Waters) with high temperature chromatograph, using 1,2,4-trichlorobenzene as the eluent at 150 ^{o}C. UV-Vis absorption spectra were recorded on a SHIMADZU UV-3600 spectrophotometer. Photoluminescence (PL) was

measured with a HORIBA FLUOROMAX-4 fluorimeter. Cyclic voltammetry (CV) was measured on a CHI660e Electrochemical Workstation equipped with a glass carbon working electrode, a platinum wire counter electrode, and a saturated calomel reference electrode. The potential of saturated calomel electrodes (SCE) was internally calibrated as 0.40 V by using the ferrocene/ferrocenium redox couple (Fc/Fc^+), which has a known reduction potential of –4.80 eV. The scan rate is 50 mV/s. Tapping-mode atomic force microscopy (AFM) images were obtained by using a Bruker Multimode 8 Microscope. Transmission electron microscopy (TEM) images were obtained using a JEM-2100F instrument. Ultraviolet photoelectron spectroscopy was measured with RIKEN KEIKI AC-3 instrument. 2D-GIWAXS measurements were performed at beamline 7.3.3 at the South China University of Technology. The 10 keV X-ray beam was incident at a grazing angle of 0.13°-0.17°, which maximized the scattering intensity from the samples. The scattered X-rays were detected using a Dectris Pilatus 2M photon counting detector. The DFT calculations was performed at B3LYP/6-31+G(d,p) level using the Gaussian 16 suite of programs.[4]

The hole-only and electron-only devices were fabricated with the architectures of ITO/PEDOT:PSS/active layer/MoO_3/Ag and ITO/ZnO/active layer/PNDIT-F3N-Br/Ag, respectively. Hole-only and electron-only devices were recorded with a Keithley 236 sourcemeter under dark. The hole and electron mobility was determined by fitting the dark current to the model of single-carrier SCLC, which is described by the equation,

$$J = \frac{9}{8}\varepsilon_0\varepsilon_r\mu\frac{V^2}{d^3}$$

where J is the current density, μ is the zero-field mobility, ε_0 is the permittivity of free space, ε_r is the relative permittivity of the material, d is the thickness of the active layers, and V is the effective voltage. The effective voltage was obtained by subtracting the built-in voltage (V_{bi}) and the voltage drop (V_s) from the series resistance of the whole device except for the active layers from the applied voltage (V_{appl}), $V = V_{appl} - V_{bi} - V_s$. The hole and electron mobilities can be calculated from the slope of the $J^{1/2}$-V curves.

Device Fabrication and characterization

The conventional structure of ITO/PEDOT:PSS/active layer/PNDIT-F3N-Br/Ag was used to fabricate the all-PSCs devices. The indium tin oxide (ITO) substrates were cleaned by sequentially

sonication with detergent, deionized water, and isopropanol. After dried in oven at 80 °C overnight, the substrates were treated with an oxygen plasma for 5 min and then coated with PEDOT:PSS (CLEVIOS PVP Al 4083) at 3500 rpm for 30 s. Annealing at 150 °C on a hot plate in air for 15 min gave a thin film of about ～40 nm. Then the substrates were transferred into a N_2 protected glove box. The active layers were obtained by spin-coating the chloroform (CF) blend solution containing chloronaphthalene (CN) additive with the total concentration of 9 mg mL^{-1}. The optimal film thickness of ca. 100 nm was obtained by controlling the rotate speed of ～2000 rpm. The film thicknesses were measured with a Bruker AXS Dektak stylus surface profiling system. All the active layers were thermal annealed in a hot plate for 10 min. Subsequently, ～10 nm PNDIT-F3N-Br as cathode interface was spin-coated onto the active layers. Finally, 100 nm Ag for opaque devices and Au (1 nm) / Ag (12, 14 or 16 nm) for semitransparent devices were thermally deposited on top of the interface through a shadow mask in a vacuum chamber at a pressure of 3×10^{-7} torr. The AVT was calculated based on the wavelength range of 380～740 nm. The effective area of the device was confined as 0.04 cm^2 or 1 cm^2 by a non-refractive mask to improve the accuracy of measurements. The current density−voltage ($J-V$) characteristics were measured under a computer controlled Keithley 2400 sourcemeter under 1 sun, AM 1.5G solar simulator (Taiwan, Enlitech SS-F5). The light intensity was calibrated by a standard silicon solar cell (certified by NREL) before the testing, giving a value of 100 mW cm^{-2} during the test of $J-V$ characteristics. The external quantum efficiency (EQE) spectra were recorded with a QE-R measurement system (Enlitech, QE-R3011, Taiwan). The transmission spectra of ST-all-PSCs were recorded with an HP 8453 spectrophotometer (Edinburgh Instruments), and air was utilized as the reference. The devices for transmittance and $J-V$ test were fabricated with the same batch and the only

di□erence was that the device for the transmittance test was evaporated without a shadow mask so that the active area covered with Ag is large enough for the test beam spot.

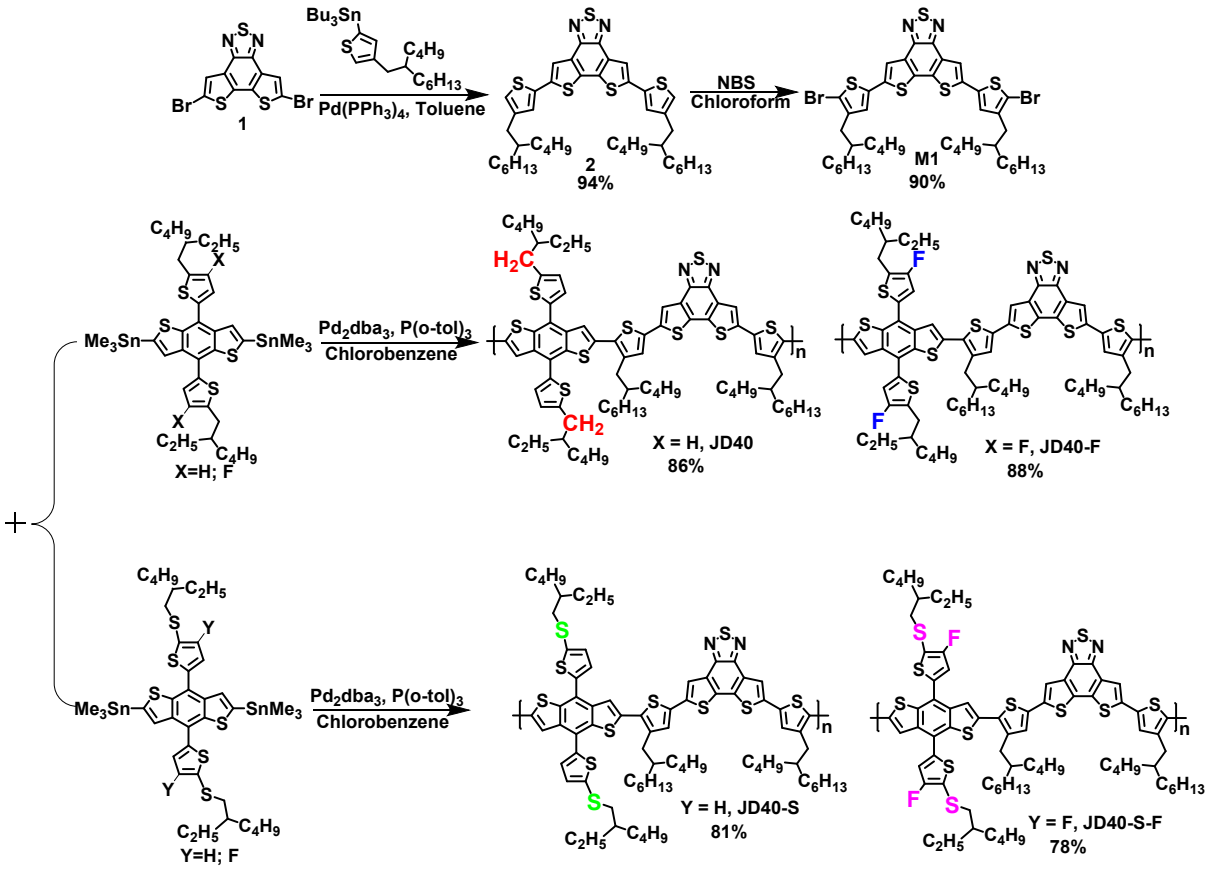

Scheme S1. Synthetic routes of the intermediates and target polymer donors

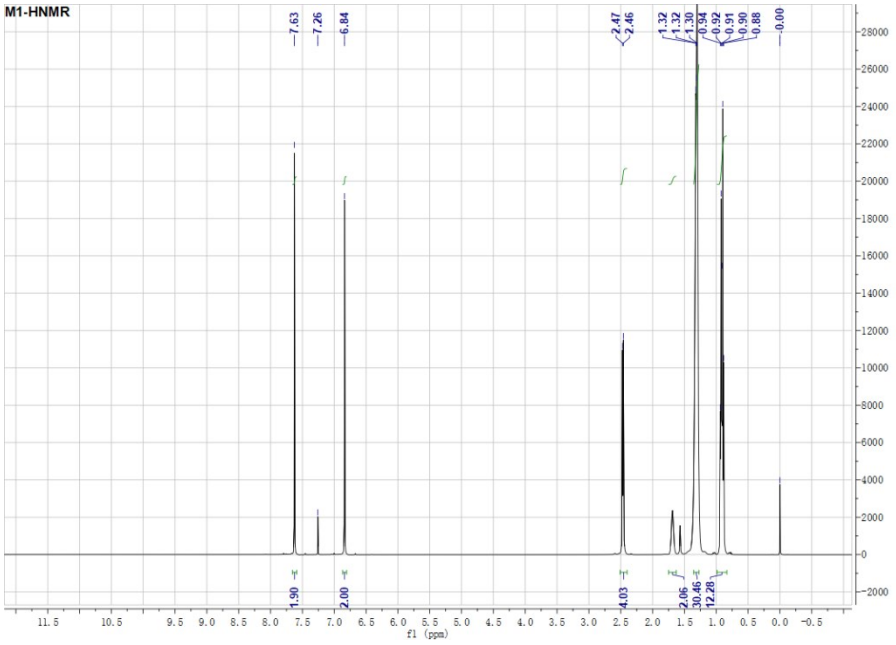

Figure S1. ^{1}H NMR spectrum of M1 in $CDCl_3$

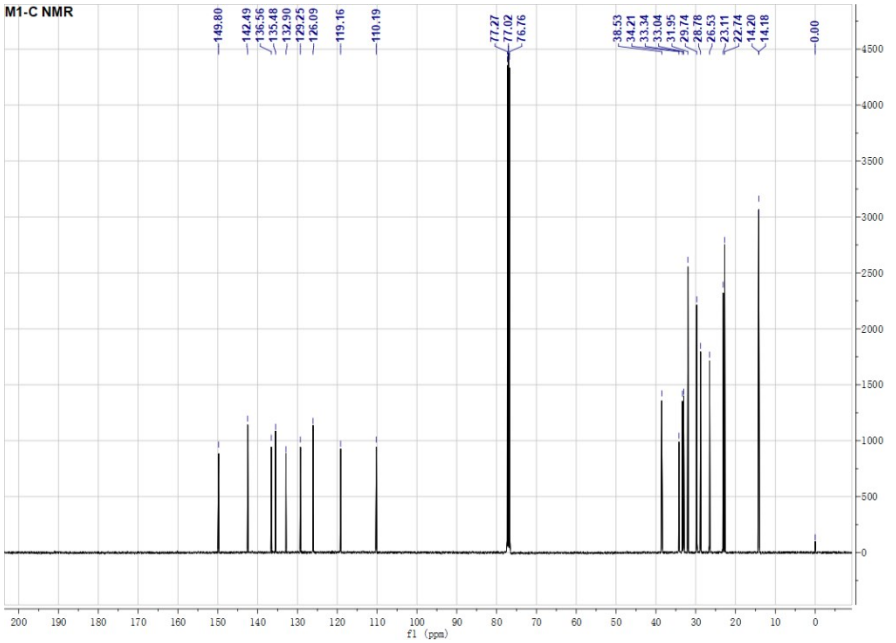

Figure S2. ^{13}C NMR spectrum of M1 in $CDCl_3$

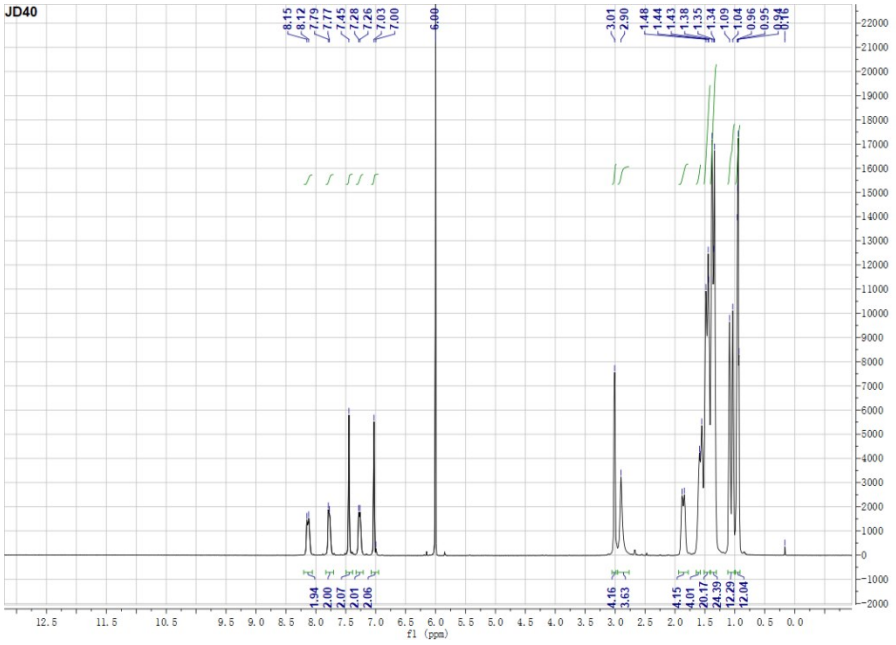

Figure S3. ^{1}H NMR spectrum of JD40 measured at 120 °C in $C_2D_2Cl_4$.

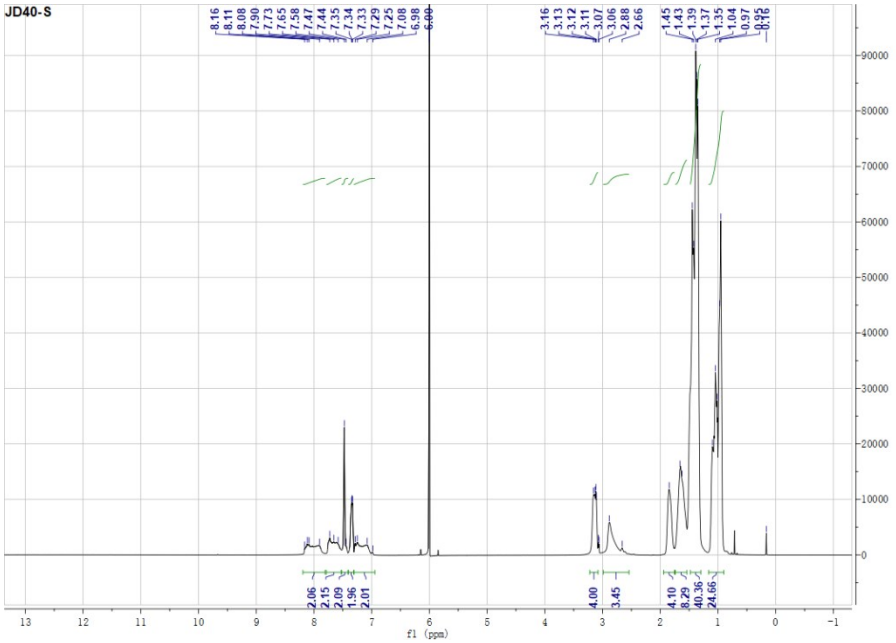

Figure S4. ^{1}H NMR spectrum of JD40-S measured at 120 °C in $C_2D_2Cl_4$.

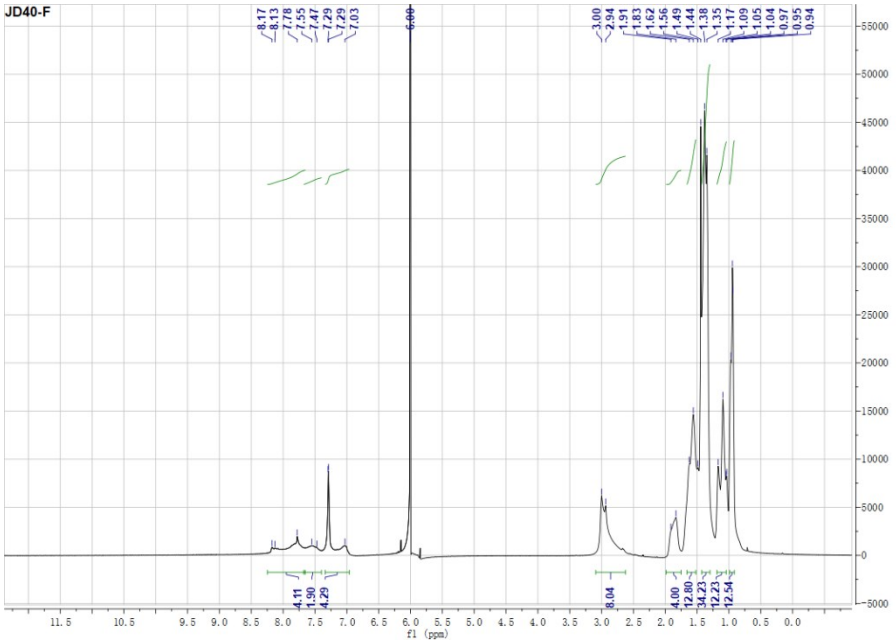

Figure S5. ^{1}H NMR spectrum of JD40-F measured at 120 ^{o}C in $C_2D_2Cl_4$

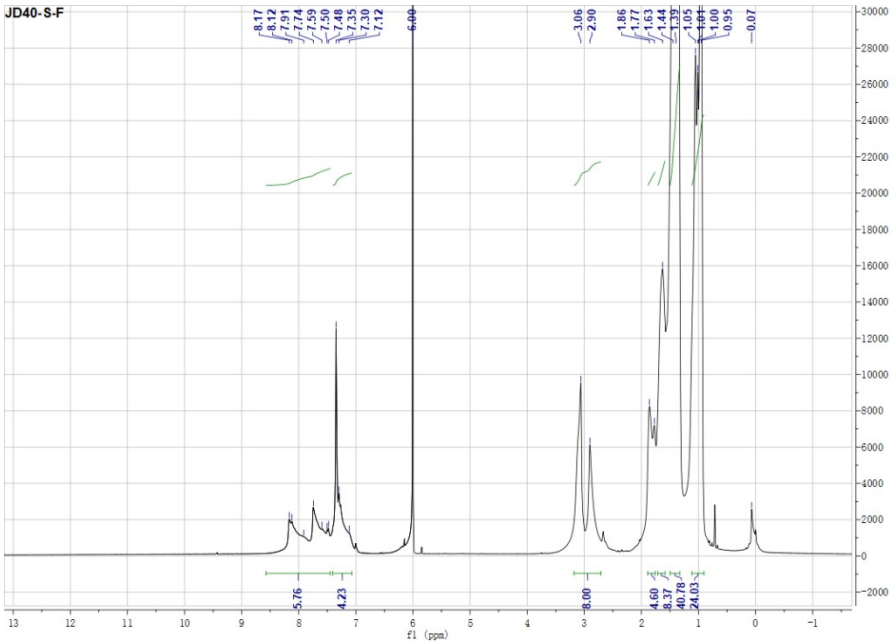

Figure S6. ^{1}H NMR spectrum of JD40-S-F measured at 120 ^{o}C in $C_2D_2Cl_4$

(a)

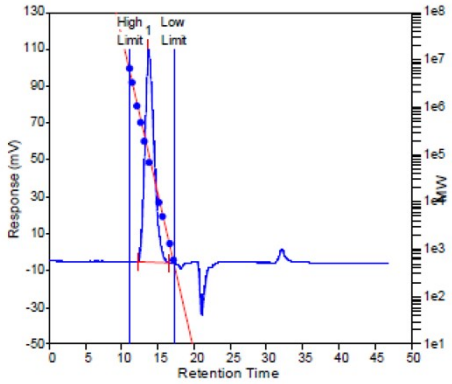

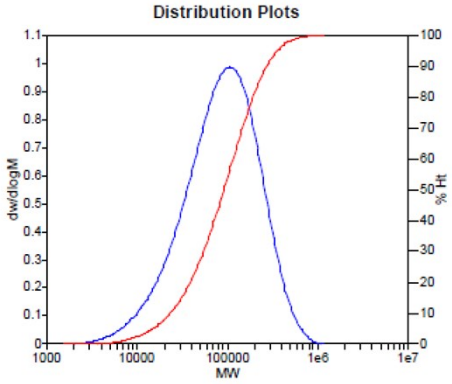

MW Averages

Peak No	Mp	Mn	Mw	Mz	Mz+1	Mv	PD
1	106680	49736	124241	228475	347056	110319	2.49801

(b)

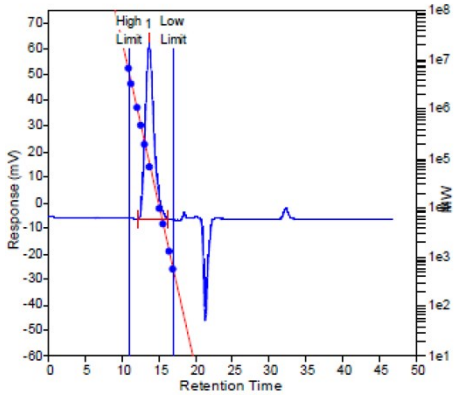

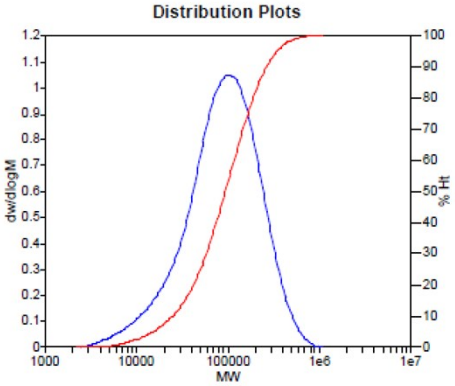

MW Averages

Peak No	Mp	Mn	Mw	Mz	Mz+1	Mv	PD
1	104002	51206	123840	219813	329060	110802	2.41847

(c)

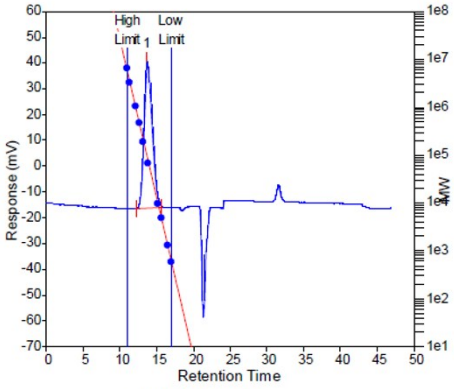

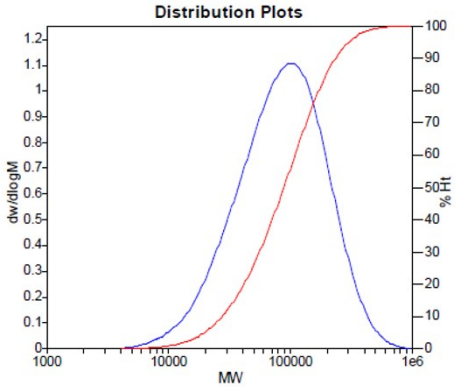

MW Averages

Peak No	Mp	Mn	Mw	Mz	Mz+1	Mv	PD
1	101391	57200	112710	189459	279461	102292	1.97045

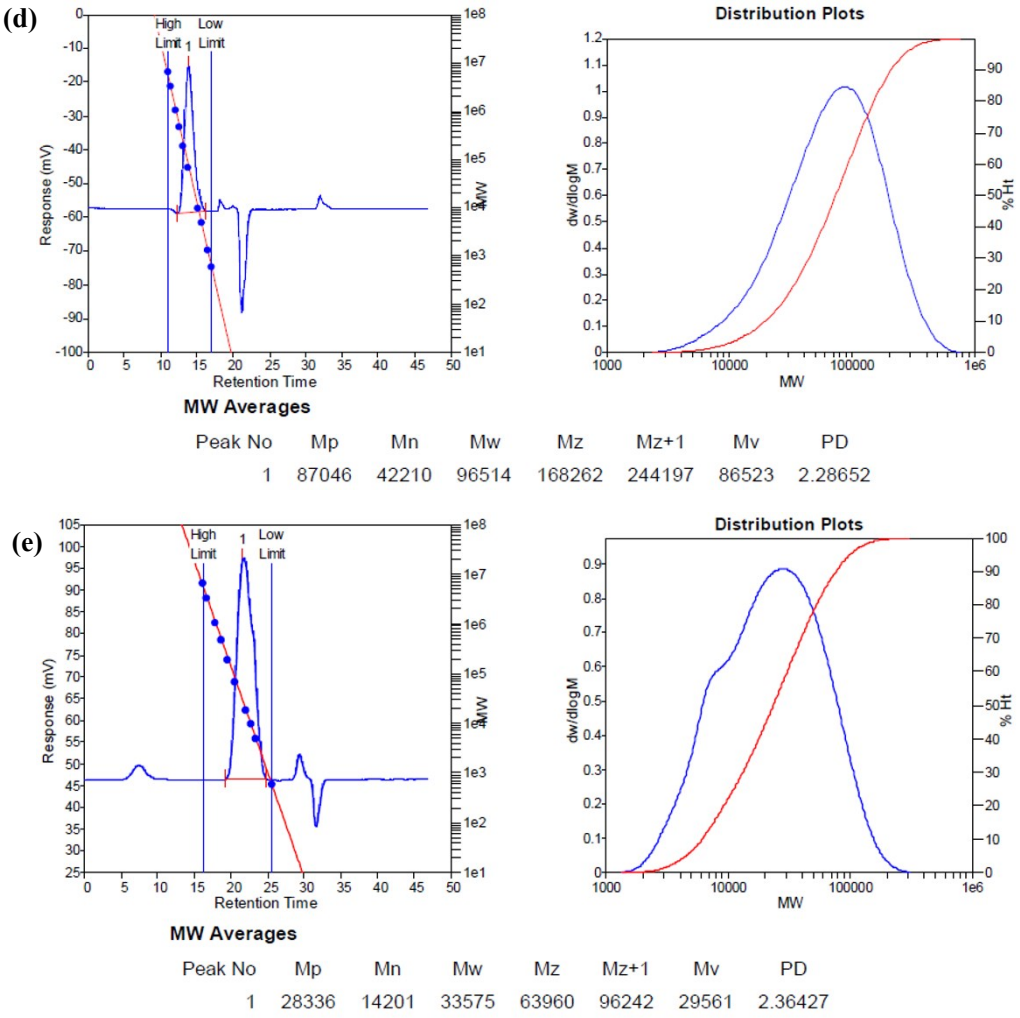

Figure S7. High-temperature GPC measurements of JD40 (a), JD40-S (b), JD40-F (c) JD40-S-F (d) and PJ1 (e).

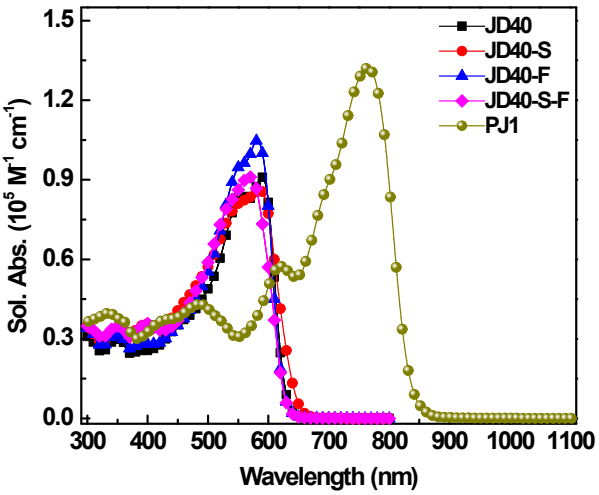

Figure S8. UV – Vis absorption spectra of the target donors and PJ1 in dilute chloroform solutions

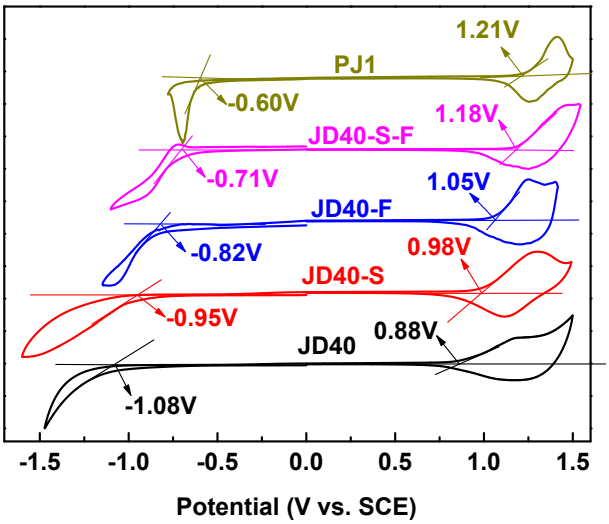

Figure S9. CV characteristics of the target donors and PJ1.

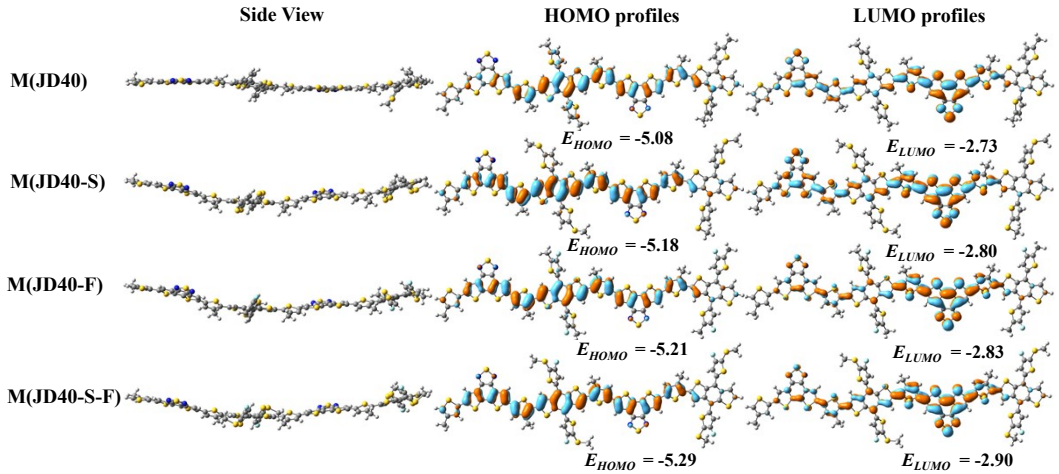

Figure S10. Optimized geometries (side view) and molecular orbitals of the simplified molecular models for the donor polymers obtained from DFT calculations

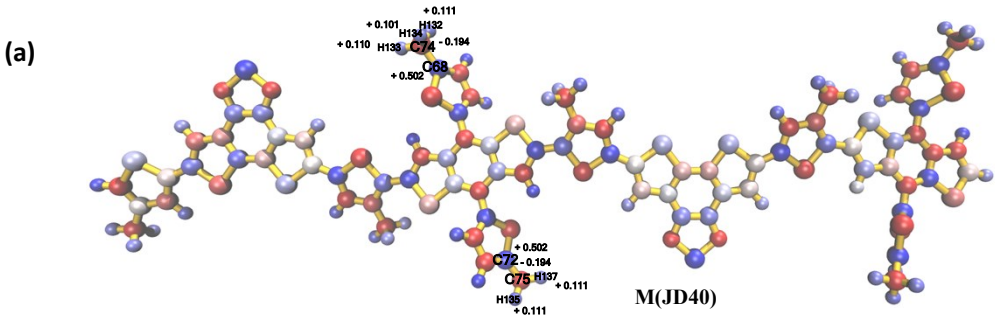

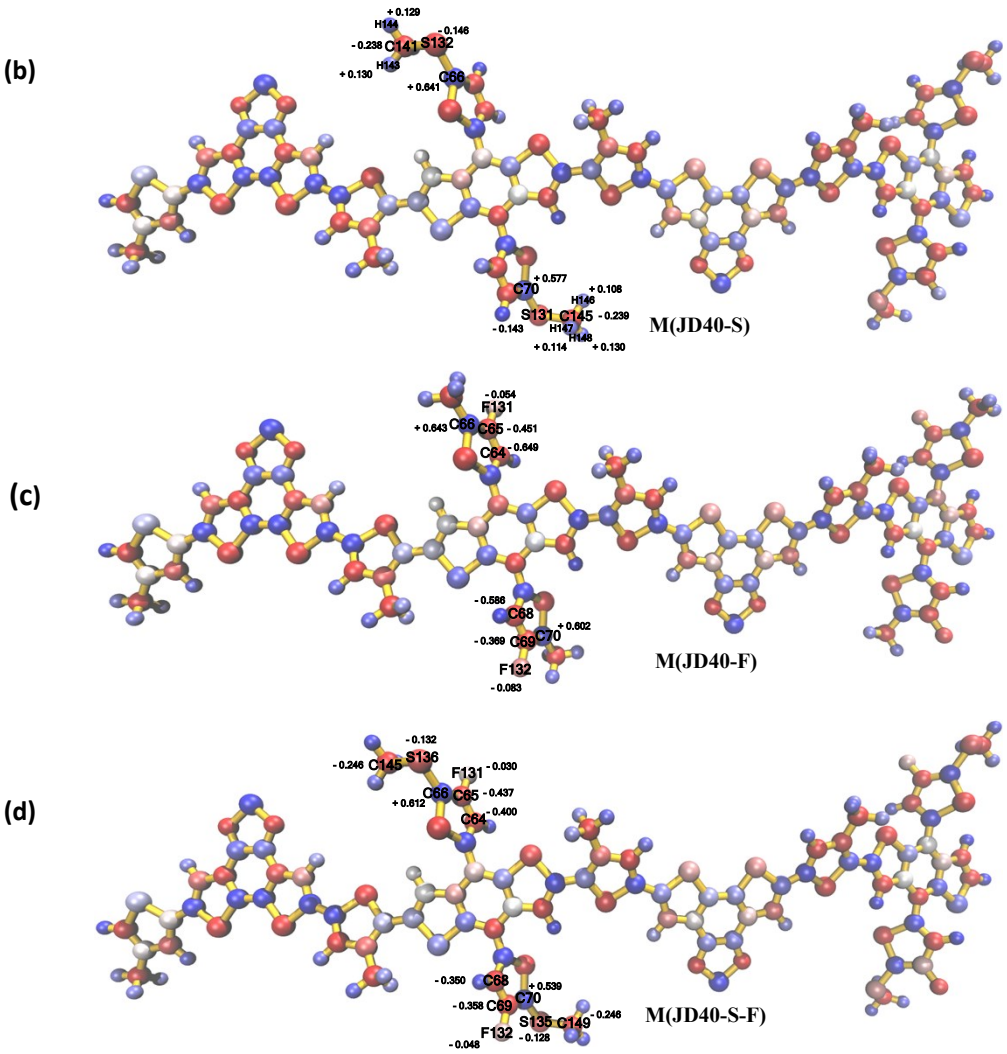

Figure S11. The atomic dipole moment corrected Hirshfeld (ADCH) charges of the simplified molecular models calculated by the Multiwfn 3.3.9 program.

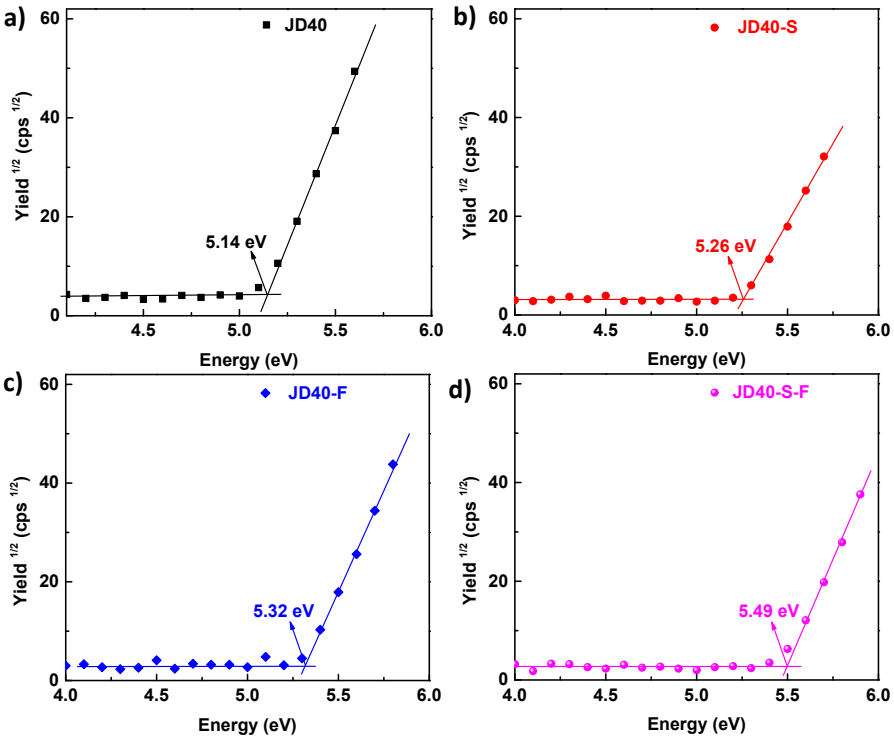

Figure S12. Photoelectron spectroscopy curves of the target donor polymers.

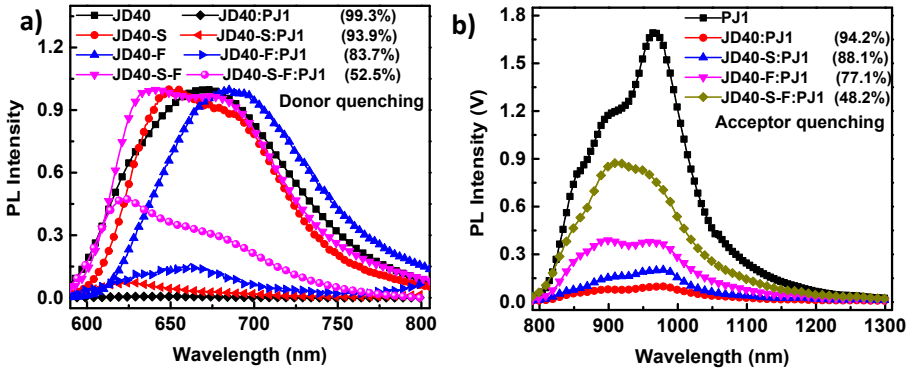

Figure S13. The PL spectra of thin films for polymer donors, PJ1 and their blends excited at (a) 560 nm for donors and (b) 760 nm for acceptor

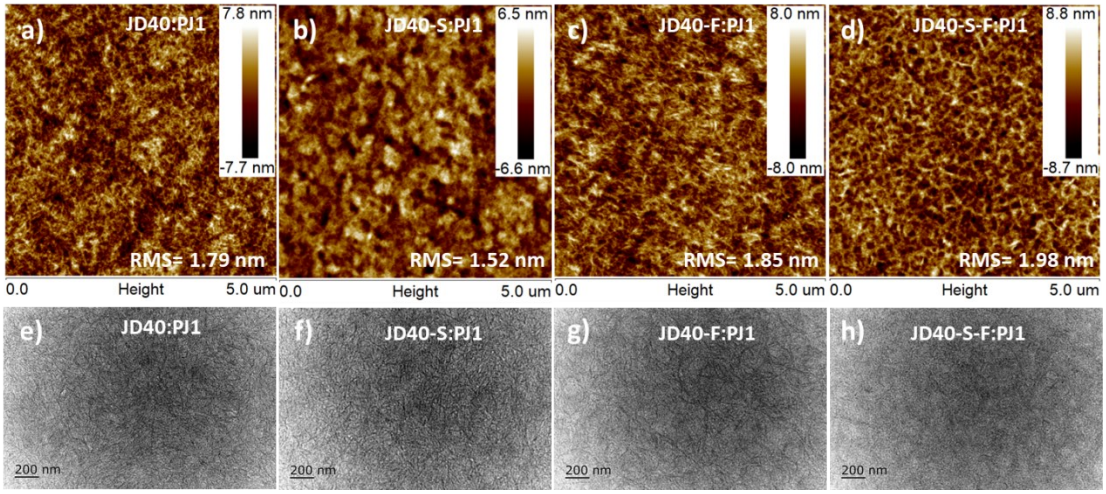

Figure S14. AFM images (a-d) and TEM images (e-h) of the blend films.

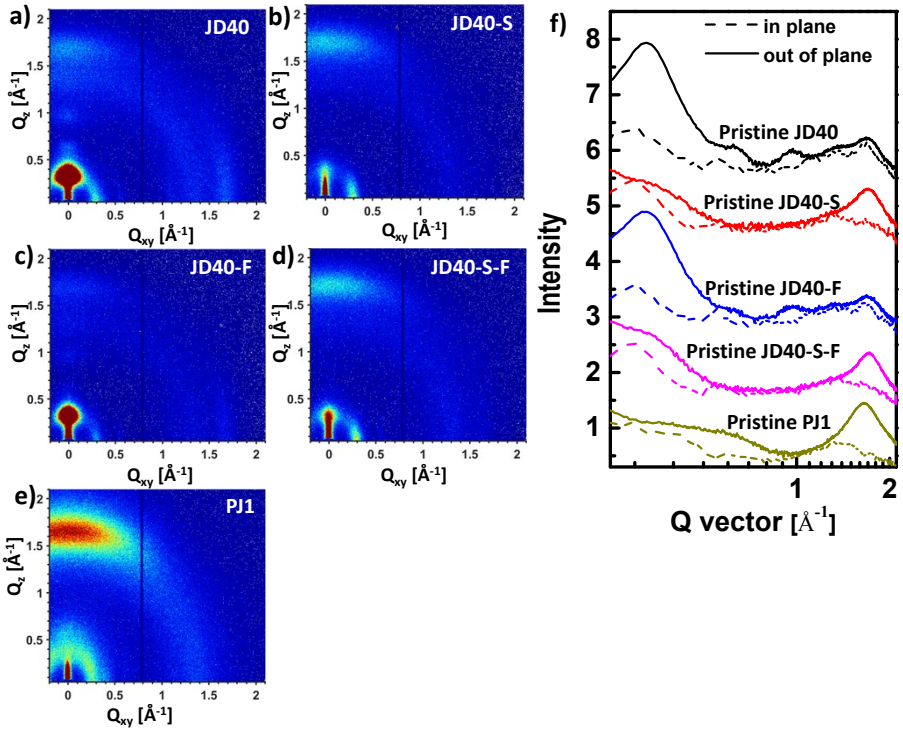

Figure S15. (a-e) 2D GIWAXS di□raction patterns of the relevant pristine films; (f) the line-cut profiles in the IP and OOP directions.

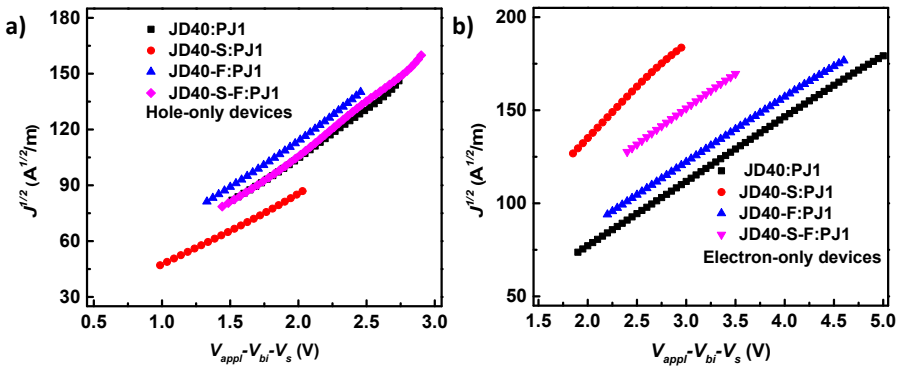

Figure S16. The $J^{1/2}$-V curves of the hole-only devices (a) with a structure of ITO/PEDOT:PSS/blend films/MoO_3/Ag and electron-only devices (b) with a structure of ITO/ZnO/blend films/PNDIT-F3N-Br/Ag according to the SCLC model.

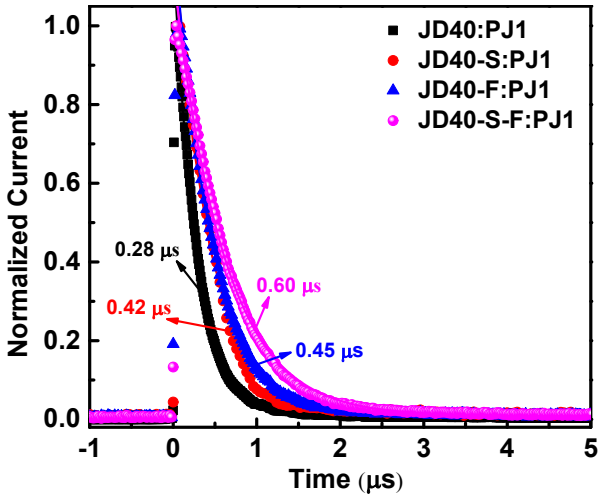

Figure S17. TPC measurements of the relevant all-PSCs at optimal conditions.

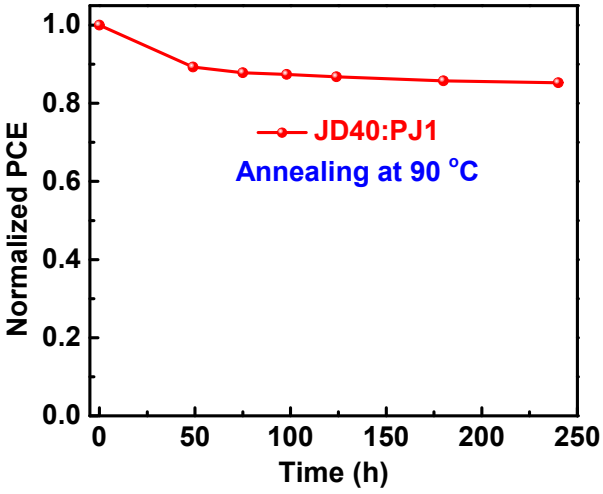

s

Figure S18. The normalized PCE of JD40:PJ1 based devices after annealing at 90 °C for different time.

Table S1. Molecular weights, UV–Vis absorption, and electrochemical properties of the target polymer donors and PJ1

Polymers	M_n (kDa)	M_w (kDa)	$\lambda_{max}^{solution}$ (nm)	λ_{max}^{film} (nm)	λ_{onset}^{film} (nm)	E_g^{opt} a) (eV)	E_{HOMO} b) (eV)	E_{LUMO} b) (eV)
JD40	49.7	124.5	580	584	648	1.91	-5.28	-3.32
JD40-S	51.2	123.8	585	587	652	1.90	-5.38	-3.45
JD40-F	57.2	112.7	581	579	645	1.92	-5.45	-3.58
JD40-S-F	42.2	96.5	569	582	643	1.93	-5.58	-3.69
PJ1	14.2	33.6	765	798	880	1.41	-5.61	-3.80

[a)] Optical bandgap estimated from the absorption onset of the thin films; [b)] Calculated from cyclic voltammetry measurements.

Table S2. Photovoltaic parameters of all-PSCs based on JD40: PJ1 at different D/A weight ratios

Condition	D/A (*w*/*w*)	V_{OC} (V)	J_{SC} (mA cm^{-2})	FF (%)	PCE (%)
CF+3%CN 9 mg/mL 100 ºC annealing for 10 min	1.5:1	0.92	21.9	71	14.4
	1:1	0.91	23.2	75	15.8
	1:1.5	0.92	22.1	74	14.9

Table S3. Photovoltaic parameters of all-PSCs based on JD40: PJ1 (1:1) with different contents of additive

Condition	Additive CN (%)	V_{OC} (V)	J_{SC} (mA cm^{-2})	FF (%)	PCE (%)
CF 9 mg/mL 100 ºC annealing for 10 min	no	0.83	22.7	65	12.2
	1%	0.89	22.1	71	13.9
	2%	0.90	22.9	73	15.1
	3%	0.91	23.2	75	15.8
	4%	0.93	22.4	71	14.8
	5%	0.92	22.5	69	14.3

Table S4. Photovoltaic parameters of all-PSCs based on JD40: PJ1 (1:1) with different annealing temperature

Condition	Annealing T (ºC)	V_{OC} (V)	J_{SC} (mA cm^{-2})	FF (%)	PCE (%)
CF+3% CN 9 mg/mL	80	0.91	22.9	72	15.1
	100	0.91	23.2	75	15.8
	130	0.91	23.1	71	15.0

Table S5. Photovoltaic parameters of all-PSCs based on JD40-S: PJ1 at different D/A weight ratios

Condition	D/A (*w*/*w*)	V_{OC} (V)	J_{SC} (mA cm^{-2})	FF (%)	PCE (%)
CF+3%CN 9 mg/mL 100 ºC annealing for 10 min	1.5:1	0.94	16.0	54	8.1
	1:1	0.95	17.1	60	9.8
	1:1.5	0.94	20.0	66	12.3
	1:2	0.94	18.5	68	11.7

Table S6. Photovoltaic parameters of all-PSCs based on JD40-S: PJ1 (1:1.5) with different contents of additive

Condition	Additive CN (%)	V_{OC} (V)	J_{SC} (mA cm^{-2})	FF (%)	PCE (%)
CF 9 mg/mL 100 ºC annealing for 10 min	no	0.93	19.6	61	11.1
	1%	0.94	21.2	69	13.7
	2%	0.94	20.2	68	13.0
	3%	0.94	20.0	66	12.3

Table S7. Photovoltaic parameters of all-PSCs based on JD40-F: PJ1 at different D/A weight ratios

Condition	D/A (*w*/*w*)	V_{OC} (V)	J_{SC} (mA cm^{-2})	FF (%)	PCE (%)
CF+3%CN 9 mg/mL 100 ºC annealing for 10 min	1.5:1	0.97	16.9	58	9.5
	1:1	0.97	17.3	62	10.4
	1:1.5	0.98	14.9	60	8.7

Table S8. Photovoltaic parameters of all-PSCs based on JD40-F PJ1 (1:1) with different contents of additive

Condition	Additive CN (%)	V_{OC} (V)	J_{SC} (mA cm^{-2})	FF (%)	PCE (%)
CF 9 mg/mL 100 ºC annealing for 10 min	no	0.97	18.1	61	10.8
	1%	0.97	18.7	65	11.8
	2%	0.97	17.6	63	10.7

	3%	0.97	17.3	62	10.4

Table S9. Photovoltaic parameters of all-PSCs based on JD40-S-F: PJ1 at different D/A weight ratios

Condition	D/A (*w*/*w*)	V_{OC} (V)	J_{SC} (mA cm^{-2})	FF (%)	PCE (%)
CF+3%CN 9 mg/mL 100 ºC annealing for 10 min	1.5:1	0.98	2.0	31	0.6
	1:1	0.99	2.5	42	1.0
	1:1.5	0.96	2.5	32	0.8

Table S10. Photovoltaic parameters of all-PSCs based on JD40-F PJ1 (1:1.5) with different contents of additive

Condition	Additive CN (%)	V_{OC} (V)	J_{SC} (mA cm^{-2})	FF (%)	PCE (%)
CF 9 mg/mL 100 ºC annealing for 10 min	no	0.96	1.8	30	0.5
	1%	0.96	2.6	33	0.8
	2%	1.0	3.1	43	1.3
	3%	0.99	2.5	42	1.0

Table S11. Photovoltaic parameters of the devices based on different batches of donor polymers （JD40）.

Donors	V_{OC} (V)	J_{SC} (mA cm^{-2})	FF (%)	PCE (%)
Batch 1 (M_n=49.7 kDa; M_w =124.2 kDa)	0.91	23.2	75	15.8
Batch 2 (M_n=37.7 kDa; M_w =85.0 kDa)	0.91	22.7	75	15.4

Table S12. Hole and electron mobilities of the related blend films

AL	μ_h (cm^2 V^{-1} s^{-1})	μ_e (cm^2 V^{-1} s^{-1})	μ_h /μ_e
JD40:PJ1	9.04×10^{-4}	8.69×10^{-4}	1.04
JD40-S:PJ1	1.31×10^{-3}	4.75×10^{-4}	2.76
JD40-F:PJ1	1.56×10^{-3}	5.39×10^{-4}	2.89

JD40-S-F:PJ1	2.30×10^{-3}	1.67×10^{-4}	13.78

Table S13. Photovoltaic parameters of ST-all-PSCs based on JD40:PJ1 with different conditions.

Thicknesses /Ag (nm)	V_{OC} (V)	J_{SC} (mA cm^{-2})	Cal. J_{SC} (mA cm^{-2})	FF (%)	PCE (%)	PCE_{max} (%)	AVT (%)
16	0.89	19.7	19.0	72	12.2±0.2	12.4	13.7%
14	0.88	18.0	17.4	71	11.2±0.1	11.3	17.2%
12	0.88	16.4	16.0	71	10.1±0.2	10.3	21.5%

References

1. Q. S. Liu, Y. F. Jiang, K. Jin, J. Q. Qin, J. G. Xu, W. T. Li, J. Xiong, J. F. Liu, Z. Xiao, K. Sun, S. F. Yang, X. T. Zhang and L. M. Ding, *Sci. Bull.*, 2020, **65**, 272-275.

2. T. Jia, J. B. Zhang, W. K. Zhong, Y. Y. Liang, K. Zhang, S. Dong, L. Ying, F. Liu, X. H. Wang, F. Huang and Y. Cao, *Nano Energy*, 2020, **72**, 104718.

3. Z. Wu, C. Sun, S. Dong, X. F. Jiang, S. Wu, H. Wu, H. L. Yip, F. Huang and Y. Cao, *J. Am. Chem. Soc.*, 2016, **138**, 2004.

4. M. J. Frisch, G. W. Trucks, H. B. Schlegel, G. E. Scuseria, M. A. Robb, J. R. Cheeseman, G. Scalmani, V. Barone, G. A. Petersson, H. Nakatsuji, X. Li, M. Caricato, A.V. Marenich, J. Bloino, B. G. Janesko, R. Gomperts, B. Mennucci, H. P. Hratchian, J. V. Ortiz, A. F. Izmaylov, J. L. Sonnenberg, D. Williams-

Young, F. Ding, F. Lipparini, F. Egidi, J. Goings, B. Peng, A. Petrone, T. Henderson, D. Ranasinghe, V. G. Zakrzewski, J. Gao, N. Rega, G. Zheng, W. Liang, M. Hada, M. Ehara, K. Toyota, R. Fukuda, J. Hasegawa, M. Ishida, T. Nakajima, Y. Honda, O. Kitao, H. Nakai, T. Vreven, K. Throssell, J. A. Montgomery, Jr., J. E. Peralta, F. Ogliaro, M. J. Bearpark, J. J. Heyd, E. N. Brothers, K. N. Kudin, V. N. Staroverov, T. A. Keith, R. Kobayashi, J. Normand, K. Raghavachari, A. P. Rendell, J. C. Burant, S. S. Iyengar, J. Tomasi, M. Cossi, J. M. Millam, M. Klene, C. Adamo, R. Cammi, J. W. Ochterski, R. L. Martin, K. Morokuma, O. Farkas, J. B. Foresman, and D. J. Fox, Gaussian 16, Revision A.03, Gaussian, Inc., Wallingford CT, 2016.